# Regional Synthesis of Mediterranean Atmospheric Circulation During the Last Glacial Maximum

J. Kuhlemann,[1]* E. J. Rohling,[2] I. Krumrei,[1] P. Kubik,[3] S. Ivy-Ochs,[4] M. Kucera[1]

Atmospheric circulation leaves few direct traces in the geological record, making reconstructions of this crucial element of the climate system inherently difficult. We produced a regional Mediterranean synthesis of paleo-proxy data from the sea surface to alpine altitudes. This provides a detailed observational context for change in the three-dimensional structure of atmospheric circulation between the Last Glacial Maximum (LGM, ~23,000 to 19,000 years ago) and the present. The synthesis reveals evidence for frequent cold polar air incursions, topographically channeled into the northwestern Mediterranean. Anomalously steep vertical temperature gradients in the central Mediterranean imply local convective precipitation. We find the LGM patterns to be analogous, though amplified, to previously reconstructed phases of enhanced meridional winter circulation during the Maunder Minimum (the Little Ice Age).

Mediterranean climate is determined by an interplay between atmospheric and marine processes and strongly differentiated regional topography (*1*). A wealth of paleoclimate data is available from archives recording conditions at the sea surface and on land at various altitudes, making the Mediterranean one of the few regions in the world where the thermal and dynamical structure of the lower atmosphere could be reconstructed for certain past intervals (*2*). Such reconstructions are invaluable for validation of the atmospheric component in climate models (*3*). Recent attempts to compare model simulations with regional proxy data over Europe during the Last Glacial Maximum (LGM) revealed substantial disagreement, both among the models and between models and paleodata (*4*, *5*), highlighting the need for model-independent constraints on past regional climatic patterns.

The state of the atmosphere in the past is inherently difficult to reconstruct. Proxies from oceanic sediments record mainly large-scale atmospheric patterns (*6*); and terrestrial proxy data, such as those from peat bogs or lake sediments, can be biased by local climate, including temperature inversion and interannual variability (*7*, *8*). The equilibrium line altitude (ELA) of glaciers contains information on the vertical structure of the atmosphere, which can be reconstructed by in situ dating of glacial advances and retreats. Small temperate glaciers in circum-Mediterranean mountain chains are (and were) exposed to well-mixed air masses and are known to have been sensitive to even small changes of the ELA, typically responding by advancing or retreating within periods ranging from several years to decades (*9*, *10*).

The ELA responds to both temperature and precipitation change (*9*, *10*), and it is possible to differentiate between these two factors only in particularly well-studied regions, such as Corsica (data supplement S1 and figs. S2 and S3). For Corsica, we present new information on the LGM ELA, including a deconvolution of the two main controlling processes (fig. S4, B and C). For the ELA depression of LGM glaciers in the wider Mediterranean region, we used previously published information (table S2), which, as a first-order end-member solution, we calculated as pure temperature change, using a standard free atmospheric lapse rate of a 6.5°C decrease per kilometer (6.5°C/km) of increasing elevation. The potential overprint of precipitation changes was then considered where anomalous results were found. The error ranges on the resultant ELA reconstructions (Fig. 1) amount to up to ±100 m in Corsica and ±150 m in other Mediterranean mountains (fig. S1 and Fig. 2). We thus developed a regional synthesis of glacial vertical temperature gradients in the lower atmosphere. Paleoflora-based temperature reconstructions for a variety of terrestrial sites at lower altitudes around the Mediterranean (*7*, *8*) (Fig. 2 and fig. S3) were used to validate and complement our ELA-based temperature reductions and precipitation patterns.

Next, we compared the ELA-based LGM cooling at alpine altitudes with estimates of LGM reduction of Mediterranean sea surface temperatures (SSTs) derived from the difference between long-term instrumental averages (*11*) and glacial SST reconstructions based on foraminiferal assemblages (*12*, *13*) and alkenone data (*14*) (Figs. 1 and 2). Such direct comparison between SST and ELA changes is warranted for the Mediterranean basin, where SSTs generally are closely related to air temperature and the insolation/radiation balance (*15*).

The combination of data on LGM cooling at sea level (SST proxies) and higher altitudes (ELA depression) provides direct constraints on the vertical structure of the LGM atmosphere. When comparing the temperature equivalent of the ELA depression with SST reduction in the LGM relative to the present (Fig. 2), we consider that a shift of similar magnitude would indicate a constant atmospheric lapse rate. Stronger relative reduction of SST would imply a lapse rate of less than 6.5°C/km, supporting more stable atmospheric stratification. A lesser relative SST reduction would imply a lapse rate steeper than 6.5°C/km, potentially enhancing the instability of the atmosphere, driving convection and consequent precipitation.

Our analysis (figs. S1 and S2) reveals an LGM pattern of southward-extending lobes of ELA depression in mountainous regions of Italy

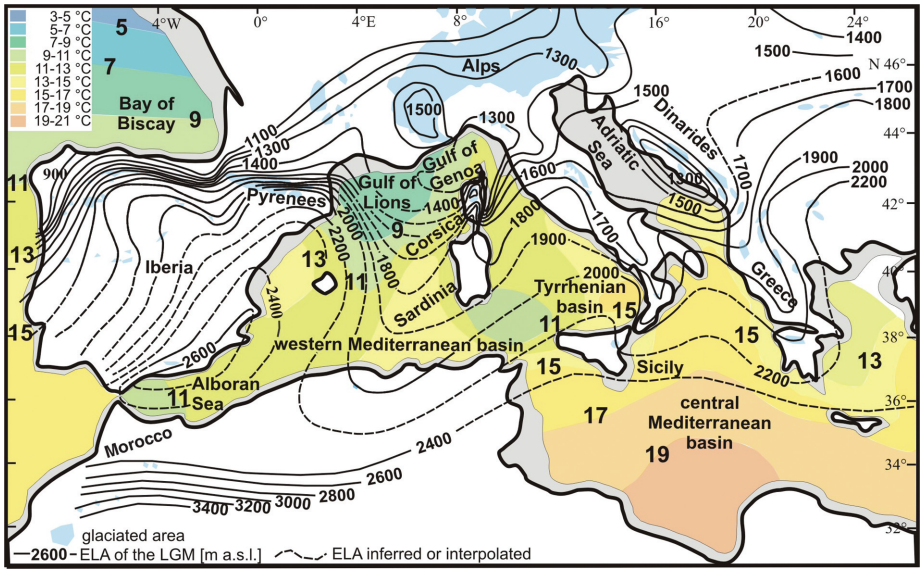


**Fig. 1.** Map of the ELA in the western-central Mediterranean region during the phase of maximum glacier expansion during the LGM (probably at ~23,000 years before the present) and of average annual SSTs and ELA during the LGM. The error range of the ELA estimate is ±150 m for the Mediterranean in general and ±100 m in Corsica.

[1]Institute for Geosciences, University of Tuebingen, Sigwartstrasse 10, D-72076 Tuebingen, Germany. [2]School of Ocean and Earth Science, National Oceanography Centre, Southampton SO14 3ZH, UK. [3]Institute of Particle Physics, HPK H30, ETH Zurich, CH-8093 Zurich, Switzerland. [4]Institute of Particle Physics, HPK H27, ETH Zurich, CH-8093 Zurich, Switzerland.

*To whom correspondence should be addressed. E-mail: kuhlemann@uni-tuebingen.de

and the Dinarides, which suggests frequent higher-altitude southward advances of polar air (Fig. 1). Iberia is characterized by a steep gradient from the northern and northwestern coastlines toward the interior and southeast, which probably results predominantly from barrier effects of near-coastal mountain ranges (Fig. 1). The data from Corsica especially identify a lobe of ELA depression that extends over the Gulf of Lions toward the south and east (Fig. 1), indicating a substantial invasion of polar air from the north. The temperature difference inferred from the recent ELA (*16*) and our LGM reconstruction (fig. S3) generally decreases from north (10° to 11°C) to south (6° to 7°C) (Fig. 2), in agreement with previous reconstructions of a steeper glacial meridional temperature gradient (*16*, *17*). The temperature differences calculated from the glacial ELA depression, relative to the present, generally agree with lower-altitude temperature reconstructions from paleofloral data (*7*, *8*) (Fig. 2).

The present-day SST distribution and surface circulation in the western Mediterranean basin are strongly affected by northwesterly winds, particularly in the Gulf of Lions (*15*). As a consequence, cool waters are frequently upwelling in the Gulf of Lions (*11*, *18*). Surface currents are deflected by coastlines, and their strength and flow direction vary seasonally in response to surface winds and the superimposed atmospheric circulation (*11*, *15*). Glacial SST values calculated from foraminiferal assemblages (*12*, *13*) and alkenone data (*14*) display a roughly similar distribution to that of modern SSTs, albeit with a stronger west-east gradient due to stronger cooling in the northwestern Mediterranean than in the central and eastern parts of the basin (*12*) (Fig. 1 and data supplement S3). The extraordinary cooling centered on the Gulf of Lions suggests frequent and/or more persistent northerly incursions of cold polar air, probably channeled through the Rhone valley at low elevation (*14*, *18*), and between the glaciated Alps and the Pyrenees at higher elevation, as suggested by our ELA reconstructions.

Figure 2 compares the spatial pattern of the LGM reduction of SST (relative to the present) with that of atmospheric temperature as derived from our ELA reconstruction. This reveals that both SST and ELA-determined atmospheric temperatures ($T_{ELA}$) underwent similar (within ±2°C) changes, relative to the present, across the northern Bay of Biscay and the western sector of the western Mediterranean. LGM SST seems less reduced than $T_{ELA}$ in the Atlantic Ocean offshore of Iberia and Morocco, which probably reflects the southward displacement of the relatively warm Gulf Stream during glacial times (*3*–*6*, *13*, *19*). In the central and (to a lesser extent) eastern Mediterranean, glacial SST appears to have dropped considerably less than $T_{ELA}$ (Fig. 2). The notable warm anomaly in the central basin can hardly be attributed to the advection of warm surface waters from the western basin because of land barriers. In fact, a notable cool SST anomaly is seen to the southeast of Sardinia, which may reflect leeward upwelling triggered by northwesterly winds (Fig. 1). We propose that the advection of warm desert air from the Sahara and relatively cloud-free subtropical conditions over the central/eastern basin largely account for the minor LGM cooling of SSTs in this region. The fact that glacial SST dropped considerably less than calculated $T_{ELA}$ over part of the Mediterranean suggests that the atmospheric lapse rate had noticeably steepened: up to ~10°C/km north of Corsica, ~9°C/km in the southern Adriatic Sea, and ~8.5°C/km in the central Mediterranean basin. Given that we applied an initial end-member ELA transformation to (only) temperature changes, using a standard lapse rate of 6.5°C/km, it is clear that increased convective precipitation must be inferred to explain the noticeably steeper rates diagnosed in these specific regions.

The spatial distributions of SST, $T_{ELA}$, and of the SST-$T_{ELA}$ difference in the western-central Mediterranean during the LGM are found to be roughly similar to those in the present, although meridional gradients were enhanced during the LGM (Figs. 1 and 2). Hence, it is not unreasonable to expect that cyclones followed similar preferential storm tracks across the basin as well, which contrasts with previous suggestions of northeast-directed cyclone tracks from the Alboran Sea toward the southern flank of the Alps (*20*). During cold periods such as the LGM, cold northerly air outbreaks over the western basin were probably more frequent (*12*, *17*, *18*). The pronounced southward cold (polar air) expansion toward northwest Africa (Figs. 1 and 2) would have triggered cyclogenesis over the relatively warm Mediterranean waters, causing flows of desert air toward the north and northeast, as indicated by the north-extending lobe of the ELA in southeastern Europe (Fig. 1). This would be consistent with observations of enhanced wind-blown dust supply from the Sahara into the eastern Mediterranean during glacial times (*21*).

Even though we compare glacial conditions (the LGM) with interglacial conditions (the present), we observe that the reconstructed property distribution patterns, particularly the preferential flow of polar air masses, are pervasive through time (Figs. 1 and 2). Indeed, these features appear to be strongly fixed by the land/sea distribution and topography, which are virtually invariant on the time scales considered. Outbreaks of polar air masses over the western Mediterranean are typically funneled between the Alps and the Pyrenees, both at present and during the LGM, causing conditions conducive to cyclogenesis over the Gulf of Genoa. The funneling effect may have been stronger with glaciated mountains, as the ice rose several hundreds of meters above the lower watersheds (*20*), and Arctic air masses would also have invaded the western Mediterranean more frequently and/or persistently than today, because of the more southerly position of the polar front during the LGM (*3*–*5*, *19*, *22*). The incursion of cold air masses would have favored the convection of moist air, especially in regions with relatively warm (less reduced) SST, so that we would predict considerable local LGM precipitation in Corsica, the Apennines, the Dinarides, and Greece, especially at the upwind flank of mountain ranges and close to the coast. This would be a suitable mechanism to explain steeper horizontal precipitation gradients during the LGM relative to the present, which indeed are suggested by our data for the steep mountainous margins of northern

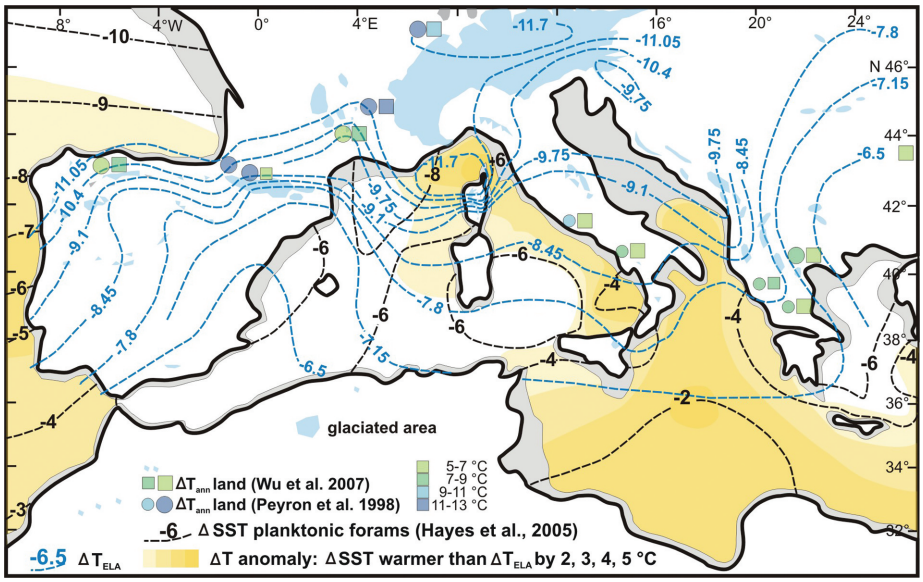


**Fig. 2.** Map of the temperature difference between recent and LGM SSTs (in black) and the temperature equivalent of the ELA depression (6.5°C/km lapse rate; in blue), respectively. The error range of this estimate is ±1°C for the Mediterranean in general and ±0.7°C in Corsica. In orange-colored marine regions, LGM SSTs were lowered significantly less than temperatures in the mid-troposphere, relative to the present. This implies an anomalously steep lapse rate and unstable layering of the lower troposphere. Atmospheric cooling values for low-elevation terrestrial sites based on paleofloral estimates are given for comparison. Small symbols indicate larger error and large symbols lesser error of the temperature estimate. Δ, change in.

Corsica (table S1 and fig. S1). This island's dry northern interior today receives ~30% less precipitation than its margins (fig. S2A), whereas this difference was ~50% during the LGM (fig. S4C). Although this prediction cannot (yet) be confirmed with the data available outside Corsica, it does agree with patterns seen in LGM reconstructions with the high-resolution climate model HadRM (*23*). As mentioned above, locally enhanced precipitation would largely reduce the local lapse rate, so that much of the initially (first-order) inferred temperature anomaly pattern in fact reflects the impact of precipitation anomalies.

Although care must be taken not to simply ascribe past regional property distributions to modern climate oscillation patterns (*24*), it remains useful to consider instrumental records and proxy data in order to develop a sense of realistic analogous climate patterns over the study region (*25*). The contrast between strongly reduced SST in the western basin and much less reduced SST in the central Mediterranean basin during the LGM (Fig. 1) indicates a preferentially meridional geostrophic circulation, with a polar trough that frequently protruded into the western Mediterranean. Such a circulation is favored by northward extension of the Azores High toward Iceland (North Atlantic ridge) or Greenland, blocking moisture supply by the westerlies. It is further enhanced by expansion and intensification of the Siberian High in winter during glacial times (*26*). A similar configuration is thought to have been common during the late Little Ice Age, notably the Maunder Minimum (*2*, *27*). The invasion of polar air as shown by our data, channeled by the topography of mountain ranges and ice sheets in Europe, would have generated cyclone formation in the Gulf of Genoa more frequently than at present, enhancing precipitation along various storm tracks in easterly directions. Our observations do not support a straightforward zonal LGM atmospheric circulation, as inferred from climate models (*19*, *28*). Instead, we propose that frequent meridional circulation during cold seasons (characterized by the LGM ELA pattern) may have alternated with more zonal circulation during warm seasons. A more comprehensive quantitative assessment of the preferential LGM atmospheric circulation requires the use of both nested model simulation and high-resolution global climate model studies (*4*, *5*, *8*, *28*), which should fully resolve the changing topography of glaciated mountain ranges and ice sheets. The validation of such models with our three-dimensional LGM climate proxy data ranging from the sea surface to alpine altitudes is a great future challenge.

### References and Notes


1. E. Xoplaki, J. F. Gonzalez-Rouco, J. Luterbacher, H. Wanner, *Clim. Dyn.* **23**, 63 (2004).
2. J. Luterbacher *et al.*, in *The Mediterranean Climate: An Overview of the Main Characteristics and Issues*, P. Lionello, P. Malanotte-Rizzoli, R. Boscolo, Eds. (Elsevier, Amsterdam, 2006), pp. 27–148.
3. COHMAP Members, *Science* **241**, 1043 (1988).
4. M. Kageyama *et al.*, *Quat. Sci. Rev.* **25**, 2082 (2006).
5. G. Ramstein *et al.*, *Clim. Past* **3**, 331 (2007).
6. G. Bond *et al.*, *Nature* **365**, 143 (1993).
7. O. Peyron *et al.*, *Quat. Res.* **49**, 183 (1998).
8. H. Wu, J. Guiot, S. Brewer, Z. Guo, *Clim. Dyn.* **29**, 211 (2007).
9. H. Kerschner, G. Kaser, R. Sailer, *Ann. Glaciol.* **31**, 80 (2000).
10. D. Steiner *et al.*, *Clim. Change,* 10.1007/s10584-008-9393-1 (2008).
11. M. Conkright *et al.*, *World Ocean Atlas 1998 CD ROM Data Set Documentation* (Technical Report 15, NODC Internal Report, Silver Spring, MD, 1998).
12. A. Hayes, M. Kucera, N. Kallel, L. Sbaffi, E. J. Rohling, *Quat. Sci. Rev.* **24**, 999 (2005).
13. A. Paul, C. Schäfer-Neth, *Palaeoceanography* **18**, 1058 (2003).
14. I. Cacho, J. O. Grimalt, M. Canals, *J. Mar. Syst.* **33-34**, 253 (2002).
15. N. Pinardi, E. Masetti, *Palaeogeogr. Palaeoclimatol. Palaeoecol.* **158**, 153 (2000).
16. B. Messerli, *Geogr. Helv.* **22**, 105 (1967).
17. V. Masson-Delmotte *et al.*, *Clim. Dyn.* **26**, 513 (2006).
18. E. J. Rohling, A. Hayes, D. Kroon, S. De Rijk, W. J. Zachariasse, *Palaeoceanography* **13**, 316 (1998).
19. M. Kageyama, F. D. Andrea, G. Ramstein, P. J. Valdes, R. Vautard, *Clim. Dyn.* **15**, 773 (1999).
20. D. Florineth, C. Schlüchter, *Quat. Res.* **54**, 295 (2000).
21. J. C. Larrasoana, A. P. Roberts, E. J. Rohling, M. Winklhofer, R. Wehausen, *Clim. Dyn.* **21**, 689 (2003).
22. U. Pflaumann *et al.*, *Palaeoceanography* **18**, 10.1029/2002PA000774 (2003).
23. A. Jost *et al.*, *Clim. Dyn.* **24**, 577 (2005).
24. F. Justino, W. R. Peltier, *Geophys. Res. Lett.* **32**, 10.1029/2005GL023822 (2005).
25. C. Cassou, L. Terray, J. W. Hurrell, C. Deser, *J. Clim.* **17**, 1055 (2004).
26. E. J. Rohling, P. A. Mayewski, P. Challenor, *Clim. Dyn.* **20**, 257 (2003).
27. J. Jacobeit, P. Jönsson, L. Bärring, C. Beck, M. Ekström, *Clim. Change* **48**, 219 (2001).
28. A. Laîné *et al.*, *Clim. Dyn.,* 10.1007/s00382-008-0391-9 (2008).


29. We gratefully acknowledge funding by the German Science Foundation (DFG project KU1298/7) and the UK Natural Environment Research Council's thematic program Quantifying the Earth System (QUEST).


### Supporting Online Material

www.sciencemag.org/cgi/content/full/1157638/DC1
Data Supplements S1 to S3
Figs. S1 to S7
Tables S1 and S2
References


11 March 2008; accepted 21 July 2008
Published online 31 July 2008;
10.1126/science.1157638
Include this information when citing this paper.


# Kinematic Constraints on Glacier Contributions to 21st-Century Sea-Level Rise


**W. T. Pfeffer,[1]* J. T. Harper,[2] S. O'Neel[3]**



**On the basis of climate modeling and analogies with past conditions, the potential for multimeter increases in sea level by the end of the 21st century has been proposed. We consider glaciological conditions required for large sea-level rise to occur by 2100 and conclude that increases in excess of 2 meters are physically untenable. We find that a total sea-level rise of about 2 meters by 2100 could occur under physically possible glaciological conditions but only if all variables are quickly accelerated to extremely high limits. More plausible but still accelerated conditions lead to total sea-level rise by 2100 of about 0.8 meter. These roughly constrained scenarios provide a "most likely" starting point for refinements in sea-level forecasts that include ice flow dynamics.**


Eustatic land ice contributions to sea-level change come from surface mass balance (SMB) losses and discharge of ice into the ocean through marine-terminating glaciers. Dynamically forced discharge, via fast flow and calving of marine-terminating glaciers allowing rapid land-to-ocean transfer of ice, is well known from studies of temperate marine-terminating glaciers (*1*–*4*) and is observed in Greenland (*5*–*7*). The consensus estimate of sea-level rise (SLR) by 2100 (0.18 to 0.6 m) that was published in the Intergovernmental Panel on Climate Change (IPCC) Fourth Assessment (*8*) excluded dynamic effects on the grounds that present understanding of the relevant processes is too limited for reliable model estimates. Because modeling (*9*) and paleoclimate comparisons (*10*) have yielded multimeter per century estimates of SLR, similar increases have been inferred as a viable 21st-century scenario. Also argued is that feedbacks unaccounted for in the IPCC estimate could quickly cause several meters of very rapid SLR (*11*, *12*).

Accurate SLR forecasts on the century time scale are imperative for planning constructive and cost-effective responses. Underestimates will prompt inadequate preparation for change, whereas overestimates will exhaust and redirect resources inappropriately. Raising California Central Valley levees only 0.15 m, for example, will cost over $1 billion (*13*); the nonlinearly increasing costs of raising levees 2 m or more without clear and compelling cause would entail enormous expenditures otherwise used for different responses as demanded by a smaller but still significant SLR.

We address the plausibility of very rapid SLR from land ice occurring this century. We give


[1]Institute of Arctic and Alpine Research, University of Colorado, Boulder, CO 80309, USA. [2]Department of Geosciences, University of Montana, Missoula, MT 59812, USA. [3]Scripps Institution of Oceanography, University of California San Diego, San Diego, CA 92093, USA.

*To whom correspondence should be addressed. E-mail: pfeffer@tintin.colorado.edu